



ELSEVIER

Available online at [www.sciencedirect.com](http://www.sciencedirect.com)

SCIENCE @ DIRECT®

Journal of Magnetism and Magnetic Materials 293 (2005) 639–646

**M** Journal of  
**M** magnetism  
**M** and  
magnetic  
materials

[www.elsevier.com/locate/jmmm](http://www.elsevier.com/locate/jmmm)

# Modelling magnetic carrier particle targeting in the tumor microvasculature for cancer treatment

Ovidiu Rotariu\*, Norval J.C. Strachan

*School of Biological Sciences, University of Aberdeen, Cruickshank Building, St. Machar Drive, Aberdeen, UK*

Available online 3 March 2005

---

## Abstract

Magnetic drug targeting of tumors situated in the cavity of the human body is difficult because the magnetic gradients decrease rapidly with the distance from the magnets. Here computer simulations are used to investigate different techniques to focus small MPs within the microvasculature of tumors. Non-invasive methods were found to have range <15 cm whilst minimal invasive methods could be applied specifically to small tumors (<18 mm).

© 2005 Published by Elsevier B.V.

*Keywords:* Magnetic drug targeting; Magnetic particles; Blood flow; Arterioles; Capillaries; Mathematical modeling; Simulation; Tumor physiology; Magnetic focusing; Magnetic needle

---

## 1. Introduction

The delivery of anticancer agents to specific target sites with minimum side effects is an important challenge in chemo-, radio- and gene-therapy. Among many existing methods, the active targeting of tumors with particulate drug carriers has gained increased interest in the last 15 years [1]. Of particular interest is drug delivery via carrier magnetic particles (MPs) of nano- and micrometre size using magnetic field gradients.

This has been demonstrated to be an efficient method to concentrate anticancer agents into tumors [2] and has achieved permanent remission of squamous cell carcinoma implanted in New Zealand White Rabbits [3]. Further, encouraging clinical trials have been performed on humans for treatment of breast cancer [4].

The study of the magnetic capture process of MPs and their release of the drug into the tumors has been comprehensively investigated for small animal models or surface tumors [5–7]. The physical aspects of the MP concentration into microvasculature have been experimentally simulated using magnetic sources positioned in the immediate proximity of the artificial blood vessels

---

\*Corresponding author. Tel.: +44 1224 272256;  
fax: +44 1224 272703.

*E-mail address:* [o.rotariu@abdn.ac.uk](mailto:o.rotariu@abdn.ac.uk) (O. Rotariu).

[8–10]. Targeting sites deep within the body has been successfully investigated for a swine model [11]. These experimental data confirm the potential of targeting only large (0.5–5.0  $\mu\text{m}$ ) iron-carbon particles into the liver of these animals, at distances <13 cm. The disadvantages in using large particles ( $\sim 5 \mu\text{m}$ ) is that they may block healthy vessels/arteries prior to reaching the tumor and may also not reach the tumor located within particular organs (e.g. brain) because they are too large to cross the endothelial barrier [12].

Focusing magnetic drug carriers requires magnetic field gradients. These magnetic field gradients drop off very steeply with the distance from the magnet. Therefore, targeting tumors at deep sites is extremely difficult. This inevitably results in poor concentration of small magnetic drug carriers (e.g. ferrofluids) within tumors hence decreasing the efficiency of treatment. However, it is very important to focus particles of reduced size specifically at the tumor, where they will have the advantage of crossing the endothelial barrier [13].

This paper presents computer simulations of minimal invasive and non-invasive methods to target small MPs at deep tumor sites within the human body. This is achieved by modelling different magnetic configurations and determining the trajectory and capture of MPs within healthy and diseased blood vessels.

## 2. Specifications

A specification of what is needed for intratumoral magnetic drug targeting was made elsewhere [5] but several additional features should be considered. The main requirements are:

- the MPs must be biocompatible and biodegradable,
- the MPs should be of an appropriate size, magnetic material and concentration that enables: sufficient attraction by the magnetic field; ease of passage into the tumor microvasculature and transmission through the endothelial tissue,
- the magnetic field should be of sufficient strength and high gradient to enable attraction and retention of the magnetic particles in the target area of either surface or deep tumors,
- the magnetic field should be adjustable in accordance with the properties of the MPs and the blood flow to avoid the MPs concentration in the normal tissue,
- magnetic targeting devices should permit the focussing of MPs within either small or large tumors,
- the MPs should contain and release an appropriate dose of anticancer agent and should be functionalised at their surface to avoid clearance by the reticuloendothelial system,
- the method of delivery should have good access to the tumor vasculature and should be minimal invasive.

In this study the following specifications of the magnets, the MPs and the blood vessels are:

*Magnets:* Three sources of magnetic field were investigated: cylindrical magnet magnetised along its diameter, magnetic circuit with parabolic shaped confocal poles (MCPSCP) and needle magnet magnetised perpendicularly on its longitudinal axis (Fig. 1). The physical and geometrical characteristics of the magnets used in the simulations are as follows:

- all magnets are made from NdFeB with an energy product of  $319 \text{ kJ m}^{-3}$  (40 MGOe);
- the direction of magnetisation ( $Ox$ ) is oriented perpendicular to the direction of the main blood vessel feeding the tumor tissue;
- the pole surfaces that come into contact with the body (tumor) have a curvature (lowest curvature—cylindrical magnet (radius  $a = 2.5 \text{ cm}$ , Fig. 1a); medium curvature—MCPSCP (pole with smallest focal parameter  $2b = 1.5 \text{ cm}$ , Fig. 1b); highest curvature—magnetic needle (radius  $a = 0.75 \text{ mm}$ , Fig. 1c));
- the curvature of the pole surface that faces the target site creates an increased magnetic field gradient. Hence, the magnetic force acting on the MPs increases and this makes possible the retention of MPs.
- cylindrical and MCPSCP magnets are larger enabling high magnetic fields ( $> 10^5 \text{ A m}^{-1}$ ) at

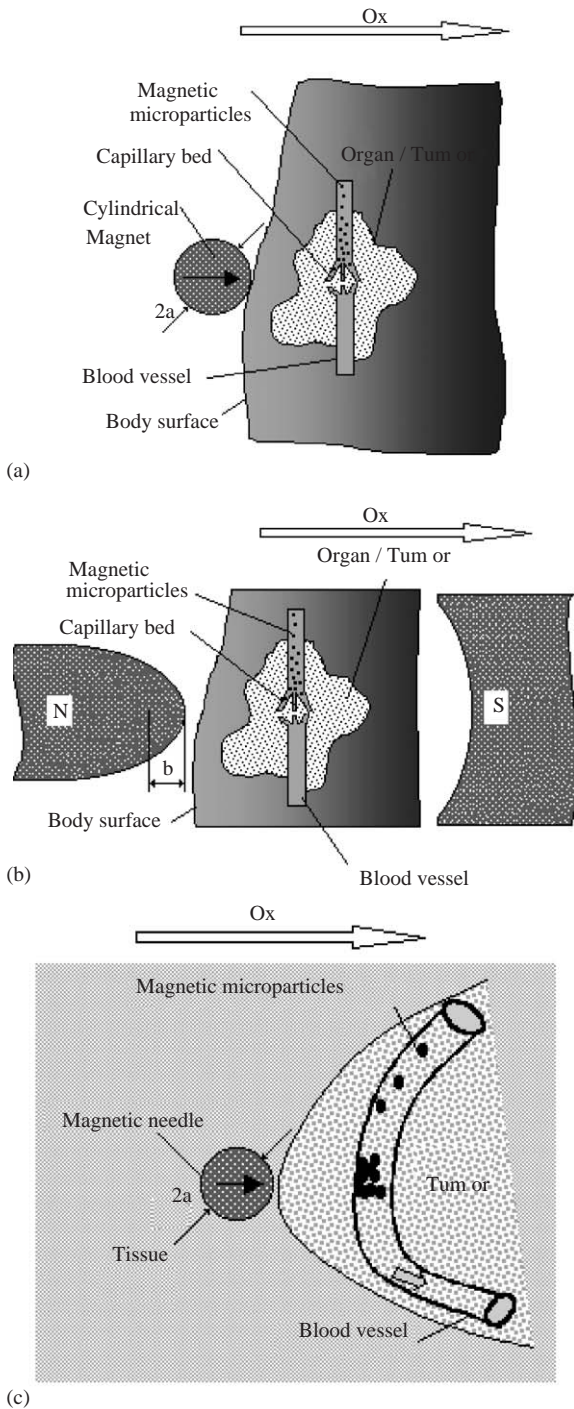


Fig. 1. Three methods for targeting MPs at a specific site inside the body: (a) using a cylindrical magnet positioned outside the body; (b) using a MCPSCP positioned outside the body and (c) using a magnetic needle inserted into the patient close to the tumor (the arrows indicate the direction of magnetisation— $Ox$ ).

distances  $>5$  cm inside the body which are essential for the efficient targeting of MPs;

- the needle magnet facilitates a high local concentration of magnetic field lines that is useful for accurate magnetic targeting in small areas.

**Magnetic particles:** The magnetic particles considered in the simulation are made of magnetite ( $Fe_3O_4$ ) with magnetisation  $M_p$  given by Langevin function (the saturation value  $= 450,000 A m^{-1}$ ). The diameter of the particles was varied between  $d = 0.1$  and  $2.0 \mu m$  that corresponds to the pore size of the tumor vasculature [1].

**Blood vessels:** Capillaries and arterioles with luminal diameters lying between  $D = 12$  and  $39 \mu m$  and lengths  $L \leq 1.0 mm$  were simulated. Blood velocity was taken to be in the range of  $0.1 mm s^{-1} < v_0 < 1.0 mm s^{-1}$  in tumors and  $1.0 mm s^{-1} < v_0 < 10.0 mm s^{-1}$  for normal capillaries and arterioles [14].

The capillaries and arterioles can have various orientations in the microcirculatory bed of tumors. However, in this study only the portions of blood vessels oriented perpendicularly to the direction of magnetisation was considered—this being the most advantageous position for particle retention/capture on the vessels' walls.

### 3. Modelling, results and discussions

The distance of capture is defined as the maximum distance between the surface of the magnet and the blood vessel where 100% of MPs are captured. In order to calculate this distance the action of magnetic and hydrodynamic forces on the MPs must be considered and the trajectories of the particles must be determined.

**Magnetic field:** The magnetic field was calculated using the 2D “Finite Element Method Magnetics” program (FEMM3.2) from Foster-Miller (<http://femm.foster-miller.com>). Fig. 2 presents 2D maps of the magnetic field (flux lines and qualitative density plot of the intensity of the magnetic field) for the cylindrical magnet magnetised along its diameter and for MCPSCP. The field's profile for the needle magnet is

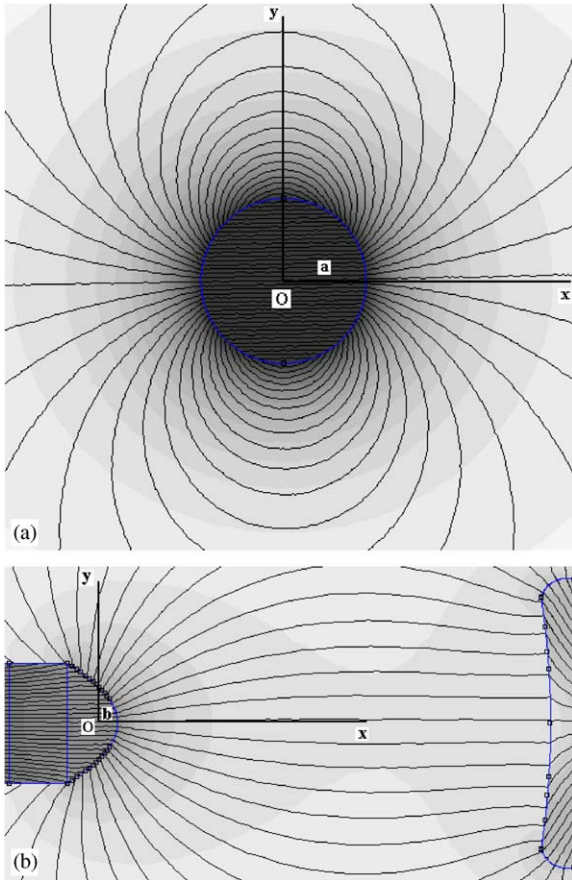


Fig. 2. 2D maps of the magnetic field: (a) cylindrical magnet (or magnetic needle) magnetised along its diameter; (b) MCPSCP (intensity of the magnetic field—grey shading).

similar with that obtained for the cylindrical magnet and is not presented. For the systems under consideration the magnetic field and gradient are highest within a range of twice the size of the pole. This is where the magnetic attractive force is largest and hence is expected to be the useful space for the magnetic capture process.

The most important component of the magnetic field for capturing MPs is in the direction of magnetisation ( $Ox$ ) of the magnet. FEMM3.2 determined the  $Ox$  component of intensity of the magnetic field  $H_x$ . A power law was fitted to these

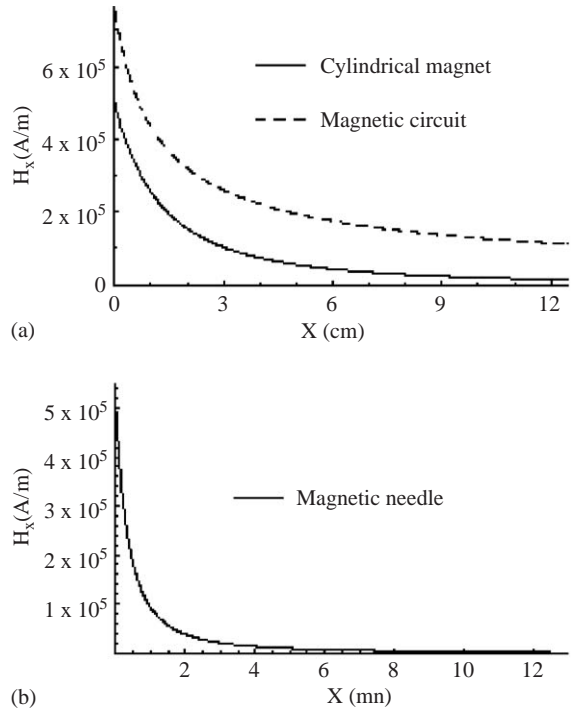


Fig. 3. The variation with distance along the  $x$ -axis of the  $H_x$  component of the intensity of the magnetic field: (a) cylindrical magnet and MCPSCP; and (b) needle magnet.

data along the  $x$ -axis. Hence

$$H_x = \frac{C_1}{x^2/a^2} \tag{1}$$

for the cylindrical magnet and the magnetic needle and

$$H_x = \frac{C_2}{(x/b)^f} \tag{2}$$

for the MCPSCP.

In Eq. (1)  $C_1 = 500\,000 \text{ A m}^{-1}$  and  $a$  the radius of the cylindrical magnet or that of the magnetic needle. In Eq. (2)  $C_2 = 760\,000 \text{ A m}^{-1}$ ,  $b$  the semi focal parameter for the smallest pole of MCPSCP and the exponent  $f = 0.67$ . The variation of the  $Ox$  component of the intensity of the magnetic field  $H_x$  vs.  $x$  is presented in Fig. 3. It can be seen that the order of magnitude of the magnetic

field is the same for both large and needle magnets ( $H \sim 10^5 \text{ A m}^{-1}$ ). But the range of action is  $\sim 10 \text{ cm}$  for large magnets whilst only  $\sim 10 \text{ mm}$  for needle magnets.

**Magnetic force:** The magnetic force acting on MPs is [15]

$$\vec{F}_M = \mu_0 V_p M_p \nabla H, \quad (3)$$

where  $\mu_0 (= 4\pi \times 10^{-7} \text{ H m}^{-1})$  is the magnetic permeability of the void space,  $V_p = \pi d^3/6$  the volume of MPs of diameter  $d$  and  $M_p$  their magnetisation.

The magnetic force acting on MPs is one order of magnitude higher for needle magnets compared with large magnets (Fig. 4). However, the range of magnetic action is only  $\sim 1.0 \text{ cm}$  for the needle magnet and  $\sim 10.0 \text{ cm}$  for large magnets. This suggests needle magnets may be useful for smaller tumors only.

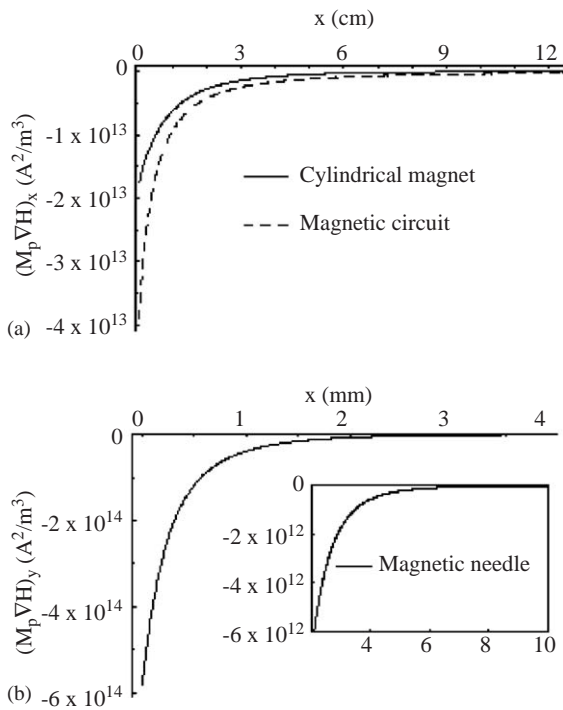


Fig. 4. The dependence of the magnetic force ( $\sim (M_p \nabla H)_x$ ) on distance along the  $x$ -axis for: (a) cylindrical magnet and MCPSCP; and (b) needle magnet (inset graph illustrates range of distance up to 10 mm).

**Flow field generated by motion of blood:** Blood flow is dependent on the architecture of tumor microvasculature. In addition, the tumors are ischemic and can have erratic blood flow [14,16] and this will influence particle capture. Also, in vivo studies of blood microcirculation show that the blood viscosity varies with its velocity [17,18]. The blood viscosity  $\eta$  is dependent on the mean velocity  $v_0$  of the blood and the diameter  $D$  of the vessels and is given by [17]

$$\eta^{1/2} = 0.032255 + 0.00087v_0^{-1/2} \quad (D = 12 \mu\text{m}), \quad (4)$$

$$\eta^{1/2} = 0.0322552 + 0.25488(v_0/D)^{-1/2} \quad (D = 23 \mu\text{m}), \quad (5)$$

$$\eta^{1/2} = 0.0344688 + 0.00202v_0^{-1/2} \quad (D = 39 \mu\text{m}). \quad (6)$$

**Hydrodynamic drag force:** Since the diameters of MPs considered here are small ( $d < 2.0 \mu\text{m}$ ) compared with the diameter of the vessels ( $D > 23 \mu\text{m}$ ) the hydrodynamic interactions between particles and vessel walls can be neglected. However, for the convenience of calculus, we keep this simple approximation for the case of smaller capillaries ( $D = 12 \mu\text{m}$ ) too, even though the capture efficiency of particles will be overestimated for this particular case. Steady flow conditions can be assumed because Reynolds number for particle motion is  $Re = \rho v_0 d / \eta \approx 0.01321$  (particle diameter  $d = 2.0 \mu\text{m}$ , blood density  $\rho = 1054 \text{ kg m}^{-3}$ , velocity  $v_0 = 10.0 \text{ mm s}^{-1}$  and viscosity  $\eta = 0.016 \text{ kg m}^{-1} \text{ s}^{-1}$ ). The hydrodynamic drag force acting on MPs can then be given by Stokes formula [19]

$$\vec{F}_D = -3\pi\eta d(\vec{v}_p - \vec{v}_0), \quad (7)$$

where  $\vec{v}_p = (dx/dt)\vec{i} + (dy/dt)\vec{j}$  is the velocity of MPs in a 2D system with  $\vec{i}$  and  $\vec{j}$  being unit vectors.

**Particles trajectories and capture distances:** Taking into account the magnetic and hydrodynamic drag forces and assuming gravity and inertia forces are negligible (small particles) the motion of MPs is given by

$$\vec{F}_M + \vec{F}_D = 0. \quad (8)$$

Combining Eqs. (1), (2), (3) and (7) in Eq. (8) gives the trajectory of the MPs for the cylindrical

magnet and the magnetic needle

$$y = \frac{v_0}{4v_{m1}a^3}(x^4 - x_0^4) + y_0 \tag{9}$$

and for the MCPSCP

$$y = \frac{v_0}{(2+f)v_{m2}b^{1+f}}(x^{2+f} - x_0^{2+f}) + y_0. \tag{10}$$

The “magnetic velocity” in Eqs. (9) and (10) is given by

$$v_{m1} = \left( \frac{\mu_0 d^2 M_p C_1}{9\eta a} \right) \tag{11a}$$

and

$$v_{m2} = \left( \frac{f\mu_0 d^2 M_p C_2}{18\eta b} \right). \tag{11b}$$

This velocity is defined as the terminal velocity of the MPs under the action of magnetic and drag forces [20]. Here the blood viscosity depends on the velocity of the blood and the diameter of the vessel (Eqs. (4)–(6)).

The trajectories of the MPs under the action of the magnetic and hydrodynamic forces are calculated using Eqs. (9) and (10). Typical trajectories of the MPs are presented in Fig. 5 for arteriole of length  $L = 1.0$  mm (equivalent to 30 times the vessel diameter [17]). All particles are captured in

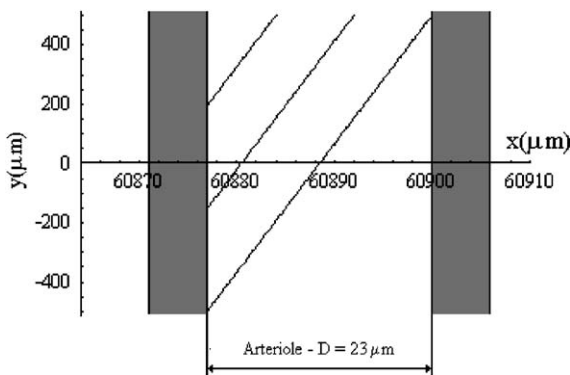


Fig. 5. Typical trajectories calculated using Eq. (9) for MPs of diameter  $d = 1.0 \mu\text{m}$  within an arteriole of diameter  $D = 23 \mu\text{m}$  and length  $L = 1.0$  mm. The arteriole is positioned at a distance  $x = 6.0844$  cm from the surface of the cylindrical magnet and the MPs start from various initial positions ( $x_0 = 60900, 60892,$  and  $60884 \mu\text{m}$ ).

the example described in Fig. 5. Formally, the distance of capture for a blood vessel of length  $L$  and diameter  $D$  is calculated as the maximum distance at which the vessel is positioned from the magnetic pole surface in contact with the body’s surface or with the tumor (for magnetic needle) for which all the MPs are captured on the vessel’s wall.

Fig. 6 presents the dependence of the distance of capture vs. the velocity of the blood and particle diameter in diseased ( $v_0 < 1.0 \text{ mm s}^{-1}$ ) and normal ( $1.0 \text{ mm s}^{-1} < v_0 < 10 \text{ mm s}^{-1}$ ) blood vessels.

For cylindrical magnet it is found:

- large MPs and diseased blood vessels—the distance of capture is  $< 10$  cm for capillaries,  $< 6$  cm for small arterioles and  $< 3$  cm for large arterioles, respectively;
- large MPs and normal blood vessels—the distances of capture is  $< 6$  cm for capillaries,  $< 4$  cm for small arterioles and  $< 1.9$  cm for large arterioles, respectively;
- small MPs and diseased blood vessels—the distance of capture is  $< 1.6$  cm for capillaries,  $< 0.2$  cm for small arterioles and 0 for large arterioles, respectively;
- small MPs and normal blood vessels—particles captured just in capillaries at the surface of the body ( $< 0.5$  cm).

For MCPSCP it is found:

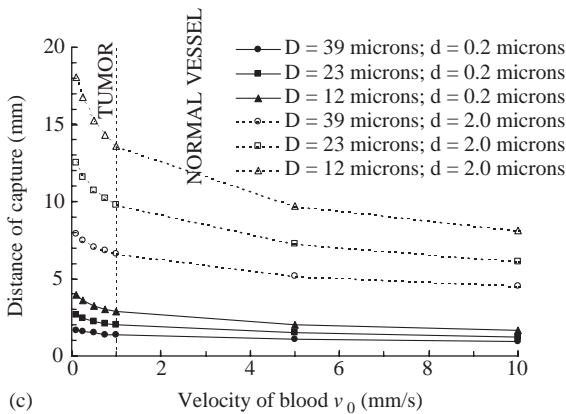
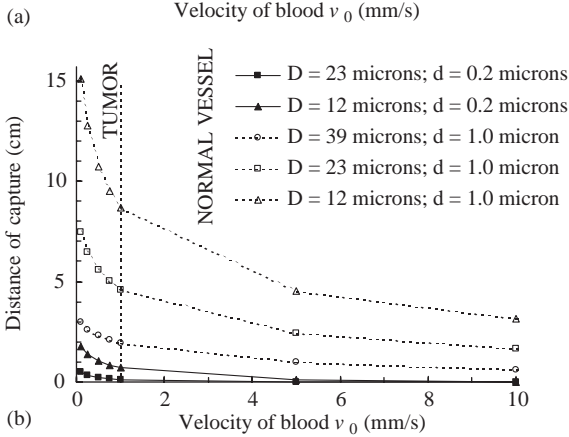
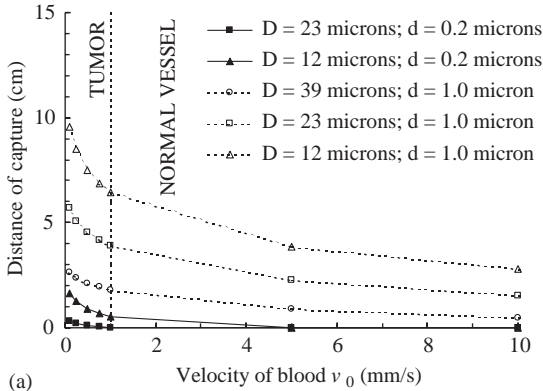
- large MPs and diseased blood vessels—the distance of capture is  $< 15$  cm for capillaries,  $< 8$  cm for small arterioles and  $< 4$  cm for large arterioles, respectively;
- large MPs and normal blood vessels—the distances of capture is  $< 8.7$  cm for capillaries,  $< 4.6$  cm for small arterioles and  $< 2.1$  cm for large arterioles, respectively;
- small MPs and diseased blood vessels—the distance of capture is  $< 1.8$  cm for capillaries,  $< 0.3$  cm for small arterioles and 0 for large arterioles, respectively;
- small MPs and normal blood vessels—particles captured just in capillaries at the surface of the body ( $< 0.7$  cm).

For needle magnet it is found:

- large MPs and diseased blood vessels—the distance of capture is  $< 18$  mm for capillaries,

- large MPs and normal blood vessels—the distances of capture is <14 mm for capillaries, <10 mm for small arterioles and <7 mm for large arterioles, respectively;

- small MPs and diseased blood vessels—the distance of capture is <4 mm for capillaries, <3 mm for small arterioles and <2 mm for large arterioles, respectively;
- small MPs and normal blood vessels—the distance of capture is <3 mm for capillaries, <2.2 mm for small arterioles and <1.5 mm for large arterioles, respectively.



#### 4. Conclusions

Computer simulations were developed to evaluate the focusing of MPs of nano- and micrometre size within tumors situated deep inside the human body. The results show that for large external magnets (cylindrical and MCPSCP) magnetite particles of diameter  $\leq 1 \mu\text{m}$  can be captured with high efficiency within the tumor capillaries and arterioles. The larger MPs ( $1 \mu\text{m}$ ) are preferentially retained at distances up to 15 cm in the capillary beds of the tumors, which have small luminal diameter and lower blood velocity than in normal blood vessels. The magnetic fields generated locally by implanting needle magnets at the tumor site focus the MPs of diameter  $\leq 2 \mu\text{m}$  in a small region ( $\sim 1$  cm) and are hence suitable for small tumors. The authors anticipate that the larger distances of capture necessary for larger tumors could be obtained using iron particles in conjunction with arrays of implanted magnetic needles, but further investigations are needed to be done.

Fig. 6. The dependence of the distance of capture on the velocity of blood flow  $v_0$  in diseased and normal blood vessels, calculated using Eqs. (9) and (10): (a) cylindrical magnet; (b) MCPSCP; (c) needle magnet. The diameters of the blood vessels and the size of MPs vary as shown ( $D = 39 \mu\text{m}$ ,  $d = 0.2 \mu\text{m}$ —full line and full circle;  $D = 23 \mu\text{m}$ ,  $d = 0.2 \mu\text{m}$ —full line and full square;  $D = 12 \mu\text{m}$ ,  $d = 0.2 \mu\text{m}$ —full line and full triangle;  $D = 39 \mu\text{m}$ ,  $d = 1.0 \mu\text{m}$ —dashed line and circle;  $D = 23 \mu\text{m}$ ,  $d = 1.0 \mu\text{m}$ —dashed line and square;  $D = 12 \mu\text{m}$ ,  $d = 1.0 \mu\text{m}$ —full line and full triangle; in Fig 6c the larger particles have  $d = 2.0 \mu\text{m}$ ). The initial coordinate  $x_0$  varied according with the position of blood vessel. The remaining parameters are as described in the main text.

## Acknowledgements

This work was funded by EU Marie Curie Fellowship (contract QLK6-CT-2002-51544).

## References

- [1] F. Marcucci, F. Lefoulon, *Drug Disc. Today* 9 (2004) 219.
- [2] U.O. Häfeli, *Int. J. Pharm.* 277 (2004) 19.
- [3] C. Alexiou, W. Arnold, R.J. Klein, et al., *Cancer Res.* 60 (2000) 6641.
- [4] A.S. Lubbe, C. Bergemann, H. Riess, et al., *Cancer Res.* 56 (1996) 4686.
- [5] C. Alexiou, W. Arnold, R.J. Klein, et al., *Cancer Res.* 60 (2000) 6641.
- [6] E. Viroonchatapan, H. Sato, M. Ueno, et al., *Life Sci.* 58 (1996) 2251.
- [7] A.S. Lubbe, C. Alexiou, C. Bergemann, *J. Surg. Res.* 95 (2001) 200.
- [8] R. Sheng, G.A. Flores, J. Liu, *J. Magn. Magn. Mater.* 194 (1999) 167.
- [9] J. Liu, G.A. Flores, R. Sheng, *J. Magn. Magn. Mater.* 225 (2001) 209.
- [10] G.A. Flores, J. Liu, *Eur. Cells Mater.* 3 (Suppl. 2) (2002) 9.
- [11] S. Goodwin, C. Peterson, C. Hoh, et al., *J. Magn. Magn. Mater.* 194 (1999) 132.
- [12] S. Jain, V. Mishra, P. Singh, et al., *Int. J. Pharm.* 261 (2003) 43.
- [13] D.J.A. Crommelin, G. Scherphof, G. Storm, *Adv. Drug Delivery Rev.* 17 (1995) 49.
- [14] R.K. Jain, *Cancer Res.* 48 (1988) 2641.
- [15] J.D. Jackson, *Classical Electrodynamics*, Wiley, New York, 1975, p. 185.
- [16] R.K. Jain, *Adv. Drug Delivery Rev.* 46 (2001) 149.
- [17] H.H. Lipowsky, S. Kovalcheck, B.W. Zweifach, *Circ. Res.* 43 (1978) 738.
- [18] A.R. Pries, T.W. Secomb, P. Gaehtgens, *Cardiovasc. Res.* 32 (1996) 654.
- [19] G.K. Batchelor, *An Introduction in Fluid Dynamics*, Cambridge University Press, London, 1970, p. 233.
- [20] J.H.P. Watson, *J. Appl. Phys.* 44 (1973) 4209.